CEAS Space Journal
https://doi.org/10.1007/s12567-024-00583-7

ORIGINAL PAPER

Analysis of sonic boom propagation and population disturbance of hypersonic vehicle trajectories

Steffen Callsen[1] · Jascha Wilken[1] · Martin Sippel[1]

Received: 18 July 2024 / Revised: 26 November 2024 / Accepted: 27 November 2024

Abstract

With more hypersonic space planes and re-entry vehicles being developed in the future, the topic of sonic boom shocks has a large impact on the feasibility of routine operations due to their impact on the ground and general population. A shockwave's sudden appearance can lead to adverse effects on the population such as being startled or experiencing sleep disturbances. Because some population overflight might be unavoidable, the sonic boom effect must be considered during the trajectory design. In this study, the trajectory design is combined with prediction methods on the sonic boom overpressure and area impact as well as the expected population response. By this, a novel approach is introduced that allows to consider the sonic boom influence already in the early design phase of a vehicle to avoid negatively impacting the population below. Trajectories of DLR's hypersonic concept called SpaceLiner are analysed as primary reference. The trajectories are optimized to avoid population overflight along the whole flight track. These analyses show that the SpaceLiner is able to avoid dense population centres on most of the investigated routes, with the number of negatively impacted people staying below 10.000 for the majority of these. Additionally, the boom propagation is compared to reference trajectories of four vehicles in the development or concept stage: Starship, Dream Chaser, Space Rider, and Aurora. Because of their shorter re-entry profile, these vehicles generally impact less area than the SpaceLiner (1–2 million km^2 instead of 2–7 million km^2). This study advances the methodology in estimating the sonic boom overpressure in the early design phase of hypersonic vehicles and how this has an effect on the population and thus routine operations.

Keywords Hypersonic vehicle · Sonic boom · Population disturbance · Trajectory optimization · SpaceLiner · Starship

Abbreviations

ANSI	American National Standards Institute
DLR	Deutsches Zentrum für Luft- und Raumfahrt e.V. (German Aerospace Center)
ESA	European Space Agency
FAA	Federal Aviation Administration
GPWv4	Gridded Population of the World, v4
IXV	Intermediate eXperimental Vehicle
NASA	National Aeronautics and Space Administration
US	United States of America

✉ Steffen Callsen
Steffen.Callsen@dlr.de

[1] German Aerospace Center (DLR), Institute of Space Systems, Robert-Hooke-Straße 7, 28359 Bremen, Germany

1 Introduction

Flying above the speed of sound leads to the creation of a shockwave phenomenon known as sonic boom which can lead to adverse effects on the general public. With the expected advent of more hypersonic space planes and re-entry vehicles in the future, these consequences must be considered in the design phase, and specifically the trajectory design, as this is critical to allow routine operations.

While the sonic boom has been an important topic for supersonic aircraft, it is often not specifically considered for hypersonic vehicles. As these often re-enter over oceans, the impact is usually not considered critical. With the arrival of reusable upper stages, the number of re-entries over populated areas is likely to increase, as they need to cross landmasses to reach a landing location close to their launch sites, which are usually located on the eastern coasts. Apart from re-entry vehicles, the sonic boom will likely be a limiting factor for any civil hypersonic point-to-point transport.

For these use cases, it will be extremely beneficial to consider the sonic boom as early as possible in the design process, so that the impact can be reduced in the ongoing design. The further along the design process progresses, the fewer changes are possible to the fundamental aerodynamic shape and trajectory design, which dictate the sonic boom response.

Current research on sonic boom for hypersonic vehicles generally focuses on the prediction of hypersonic booms, either advancing fast prediction models [2, 3] or utilizing computational fluid dynamics for precise predictions [4, 5]. Alternatively, the atmospheric impact on the sonic boom can also be a study focus [6, 7]. However, the population impact of the sonic boom is usually not considered during early-stage mission design of hypersonic vehicles.

This manuscript attempts to improve on the status quo in the early design phase by combining the trajectory design with the sonic boom prediction and then as a consequence also the estimated population response created by these booms. This approach allows the assessment and comparison of various hypersonic re-entry vehicles, with the focus being the DLR SpaceLiner concept.

Specifically, this study attempts to explore the following four questions: What is the estimated overpressure magnitude along the flight route of the reference vehicles? How is the general population impacted by these flights? How do the sonic boom propagations compare between different vehicles in this realm? And finally, what implications can be deducted from these results on the next generation SpaceLiner design?

The main reference vehicle is DLR's SpaceLiner concept design for future high-speed rocket-propelled Earth point-to-point transportation. A large number of envisioned routes are analysed regarding the sonic boom propagation, which have beforehand been optimized to avoid population centres during the trajectory design. The computation of the sonic boom propagation is achieved by using conventional estimation methods. The annoyance of the people is assessed based on population survey studies which use the overpressure as the main input. As a validation case, the Space Shuttle is the primary option with sufficient data available [8].

Finally, the SpaceLiner's sonic boom propagation is compared to the reference trajectories of four other vehicles: Starship, Dream Chaser, Space Rider and Aurora. Since the exact flight paths for these are not (publicly) known, the focus is not placed on the population disturbance, but the general characteristics of their sonic boom including impact area and overpressure magnitude.

This methodology allows the implementation of the sonic boom estimation and its effects on the general population within the early design phase, which is critical for the architecture of such vehicles.

2 Vehicle description

The vehicles selected for this study were chosen based on the available data and their relevance in future spaceflight. Because of its conception in the German Aerospace Center (DLR), the SpaceLiner allows for the most detailed analysis. Additionally, data is available for SpaceX Starship, the Dream Chaser, Space Rider as well as the Aurora spaceplane concept. Each vehicle is given a short description, but the main technical data is summarized in Table 1. With these vehicles, this study covers a broad selection of hypersonic vehicle shapes and sizes.

2.1 SpaceLiner 7–3

SpaceLiner is a concept for a high-speed Earth point-to-point passenger transport system as well as a satellite launcher internally developed at DLR (see Fig. 1) [9, 10]. It could transform ultra-long-distance travel on Earth while at the same time enable low-cost space transportation. Travel times for the longest distances (e.g. Europe – Australia) are expected to be about 90 minutes. In case of the orbital transportation system, it is designed as a fully reusable two-stage system with an additional kick stage in place of the passenger capsule. This system is described in more detail in [11].

The aerodynamic design of the SpaceLiner passenger stage enables the flight routes discussed in this study. With a high lift-to-drag ratio of up to 3.5 in the hypersonic range, its single-delta wing is optimized for high-altitude flights above 60 km. More detailed analysis of the aerodynamic and aerothermodynamic design is published in [12–15].

Table 1 Summary of vehicle parameters

	SpaceLiner passenger stage	Starship stage	Dream Chaser	Space Rider	Aurora
Length	65.6 m	50 m	9 m	4.6 m	45 m
Span	33 m	19.2 m	7 m	2.3 m	25 m
MTOW	366 t	1330 t	18 t	2.7 t	450 t
Dry mass	129 t	130 t	11 t	2.0 t	48 t
Re-entry speed	Orbital	Orbital	Orbital	Orbital	Mach 15

Fig. 1 Rendering of the SpaceLiner passenger stage in gliding flight over Alaska, US

After the passenger stage burn is completed, which is generally below 90 km altitude and Mach numbers above 20, it performs a gliding descent to the target location, primarily using its high hypersonic lift-to-drag ratio to create lift at altitudes between 60 and 80 km. During this flight phase, it can vary its angle of attack and bank angle to perform manoeuvres towards the landing site. Once it arrives at the target location, a horizontal landing on a runway is performed.

2.2 SpaceX Starship

SpaceX is currently developing the space transportation system Starship which aims to be the first ever fully reusable launcher [16]. It is a two-stage to orbit system with a reusable payload mass to low Earth orbit of around 100 tonnes. It is proposed to be refuelled in orbit and shall eventually carry humans to Mars. Additionally, it is contracted to carry humans from an orbit around the Moon to its surface within the Artemis program [17]. Furthermore, SpaceX has proposed to use Starship for point-to-point transport on Earth similar to the SpaceLiner [18]. A comparison of the point-to-point missions of these vehicles is published in [19] and a critical analysis by DLR in [20]. The upper stage called Starship shall re-enter the atmosphere and land vertically by being caught by a tower. This is the relevant part for sonic boom creation.

2.3 Sierra Space Dream Chaser

The Dream Chaser is a US-American reusable spaceplane developed by Sierra Space for commercial resupply missions to the International Space Station, which shall be launched on top of an Atlas V. About 5.5 tonnes of supply can be delivered to the ISS [21].

After staying in orbit, it re-enters the atmosphere to land horizontally on an airport runway. There have been studies in Europe whether it would be possible to land the Dream Chaser at a European spaceport like the one proposed in Rostock–Laage, Germany [22].

2.4 ESA Space Rider

The Space Rider vehicle funded by the European Space Agency (ESA) is a reusable space laboratory in the form of a lifting body. It shall be launched on top of a Vega C and stay in orbit for a few weeks or months. Once its mission is complete, it will return to Earth. After performing an atmospheric re-entry using its lifting capabilities, it lands under a parafoil [23, 24].

2.5 DLR/Polaris RFZ Aurora-R2

Aurora-R2 (in the following named Aurora) is a concept for a reusable spaceplane that shall take off horizontally from a normal airport with jet engines and later ignite rocket engines to accelerate to approximately Mach 15. At Mach 15, the second stage and payload are released from the vehicle and continue to orbit. The spaceplane re-enters the atmosphere and lands on an airport like a normal plane. The vehicle was initially developed at DLR [25] and is currently being further advanced at the DLR spin-off company Polaris Raumflugzeuge GmbH [26]. The data discussed here and shown later reflect the vehicle version R2 and does not include the further iterations done within Polaris Raumflugzeuge GmbH.

3 Methodology

The primary focus of this study is to establish a methodology which allows to study the sonic boom carpet created by hypersonic vehicle trajectories, and from that draw conclusions on the impact it will have on the general population. This data can be used in the early iterations of a vehicle design phase to reduce the expected disturbance on the population originating from vehicle operations. The creation of the trajectories is explained in the first section of this chapter and some reference trajectories are given. Furthermore, the essential sonic boom theory and how it intertwines with population disturbance studies are described in more detail in the subsequent sections. In the end, the population density database used for the analysis of the population disturbance is presented.

3.1 Trajectories

Different methodologies are used for the creation of the vehicle trajectories. The Starship and SpaceLiner are able to fly trajectories between two different points on Earth, which are more complex to compute than orbital re-entries due to the inclusion of ascent and descent phase including complex boundary conditions with regard to the overflight of the populated areas. This is why multi-objective optimization methods with evolutionary algorithms are used in this case. The method and its application are explained in more detail in [19, 27] for both vehicles. However, because Starship does not have a complex trajectory in either case, an orbital re-entry is chosen instead for simplicity. For the orbital re-entry vehicles (Starship, Dream Chaser, Space Rider), a simple guidance is sufficient to compute the re-entry trajectory.

The SpaceLiner vehicle is able to use its high lift-to-drag ratio to glide and perform manoeuvres at high speeds, which leads to significant cross-range capability. Consequently, the solution space for SpaceLiner is also substantially larger. As an example, the SpaceLiner can choose between flying a relatively direct route between two points like Starship or diverging thousands of kilometres to the left or right and still arrive at the target location if the performance permits. The latter is beneficial when larger landmasses with population are on the direct route. Thus, an annoyance due to the sonic boom can be avoided.

Because of this inherent complexity in the SpaceLiner trajectories, multi-objective optimization tools are used which allow to investigate multiple feasible routes with a focus on mitigating the population disturbance of the sonic boom, while still complying with all of the vehicle's structural and thermal constraints. It is possible to compute trajectories which minimize the population along the flight path while also reducing thermal parameters like the peak heat flux. Minimizing the overall population overflown during the flight leads to trajectories that mostly fly over scarcely populated areas like the polar regions and oceans. However, sometimes it is not possible to avoid inhabited continental landmasses, and even some ocean areas are quite populated (e.g. Oceania). For these parts of the trajectory, the sonic boom overpressure should be as small as possible.

Besides the subject of noise pollution, the factor of safety for the general population has to be considered. For the purposes of this study, it is assumed that the SpaceLiner system satisfies the safety requirements to be allowed to fly over certain populated land areas. As a passenger transport system, it inherently has to satisfy high safety requirements. However, it shall avoid highly populated areas as best as possible, which is supported by the chosen methodology. Thus, the population avoidance is primarily focused on noise pollution, with the added bonus of a safety increase.

Figure 2 shows the characteristic re-entry profile of SpaceLiner and Starship — each representing a typical vehicle architecture: high and small lift-to-drag ratios, respectively. Additionally, the Space Shuttle is depicted as a well-known reference case. The SpaceLiner is able to achieve a significantly larger distance flying in the upper atmosphere compared to other vehicles.

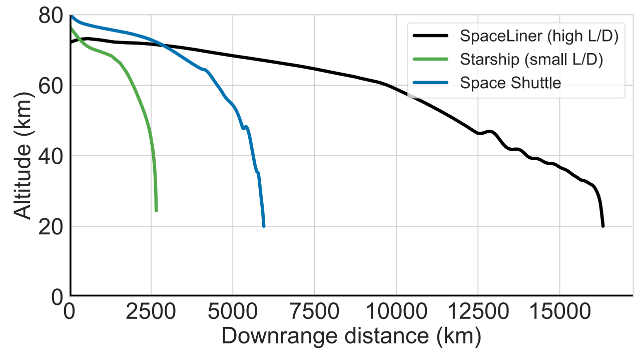

Fig. 2 Typical hypersonic re-entry trajectories

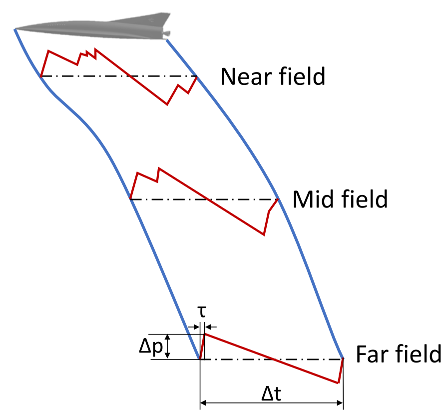

Fig. 3 Shock wave signatures from near- to far field, adapted from [1]

3.2 Theory of sonic boom and population impact

Any vehicle moving above the speed of sound creates shockwaves. These shockwaves propagate through the atmosphere and, when they reach the ground, can produce the sound phenomenon known as sonic boom, which may impact the general population, but also wildlife and buildings. This section is intended to give an overview on the propagation effects of sonic booms and their impact on human behaviour. The primary reference for this section is [1].

Far away from the vehicle, the sonic boom can generally be characterized by an N-shape pattern (see Fig. 3). It has two shock walls created by the front and back of the vehicle and a gradually declining pressure part in-between. Therefore, the N-shaped sonic boom can be classified by three parameters: the pressure difference Δp to the ambient atmosphere (also called overpressure), the rise time τ to reach the pressure peak and the time difference Δt between the bow and tail shock. Each parameter impacts the way humans react to experiencing a sonic boom.

The pressure difference Δp is mostly responsible for the perceived sound intensity and is measured in Pa. Generally, supersonic aircraft have an overpressure up to about 150 Pa. As a comparison, the Concorde created an overpressure of 93 Pa at Mach 2 and an altitude of 16 km. The time difference Δt, which is determined by the distance between the front and tail of the vehicle, determines whether the human ear interprets the sonic boom as a single sound or two separate sounds. Whether people experience a startle effect or not is mostly determined by the rise time τ. The shorter the rise time, the more sudden a sonic boom is felt and thus humans tend to react with an unpleasantly perceived startle. Also, the sensitivity of the human ear is higher in the frequency range that corresponds to the quick rise in pressure.

Generally, the sonic boom of a supersonic vehicle touches the ground in a primary and secondary carpet (see Fig. 4). The primary carpet consists of most of the downward-oriented waves and generally exhibits the highest overpressure values. There, people will possibly experience disturbance effects like startle, annoyance and loss of sleep. Additionally, there are worries about structural damage of buildings and behavioural impact on wildlife.

In this area, the sonic boom is shaped in a classical N-form. As can be seen in Fig. 5, the overpressure magnitude peaks directly below the vehicle's track and decreases laterally. The lateral decrease is steeper at first, but gets shallower towards the edge of the primary carpet.

At a certain lateral distance to the vehicle, the rays are refracted upwards away from the ground (see Fig. 6). This leads to a rather sudden primary carpet cutoff, as all further rays are refracted upwards into the atmosphere. The actual lateral distance of the cutoff primarily depends on the Mach number and altitude as it is mostly an atmospheric phenomenon.

Both the refracted rays from the ground as well as the upwards motioned rays from the vehicle hit the thermosphere where the temperature rises with increasing altitude. This leads to a general bending of the sonic boom rays towards the ground. These rays then form the secondary sonic boom carpet further towards the side. As a lot of the

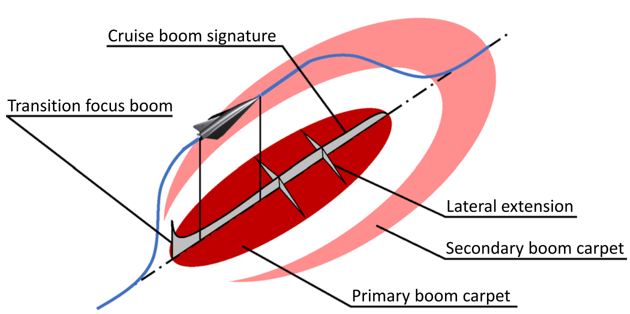

Fig. 4 Sonic boom ground propagation, adapted from [1]

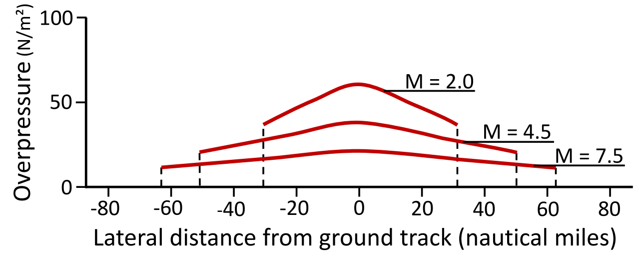

Fig. 5 Sonic boom lateral distribution for the Space Shuttle orbiter re-entry, adapted from [1]

sonic boom energy has been dissipated during the long track through the atmosphere, the sonic boom signature is more benign — overpressures below 10 Pa and high time differences of 5–10 s. Thus, the secondary carpet boom rather sounds like long, distant thunder than a sharp sonic boom.

From past studies, it is known that the continuous exposure of the sonic boom overpressures created by military vehicles, but also the Concorde is described as unbearable by a considerable number of the population. Thus, the trajectory design and optimization must at best avoid any populated areas during supersonic flight to achieve acceptance within the population. This is why civil supersonic flights are generally confined to operations over the sea.

The vehicle analysis in the subsequent chapters shows that during high-speed high-altitude flight, the sonic boom overpressure is quite low, below 20 Pa. The overpressure magnitude increases to concerning levels only in the later flight phases when flying below approximately 40 km. Thus, while still avoiding population as best as possible, some overflight at high altitude might be acceptable if the route does not allow any other option. Therefore, an overview of the studies performed on the human response will

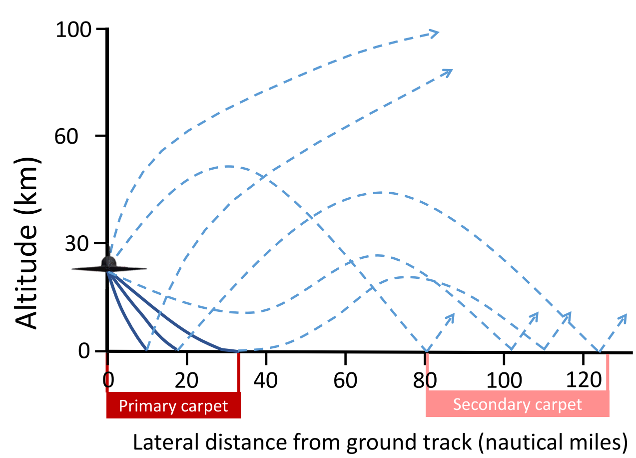

Fig. 6 Sonic boom propagation through the atmosphere, adapted from [1]

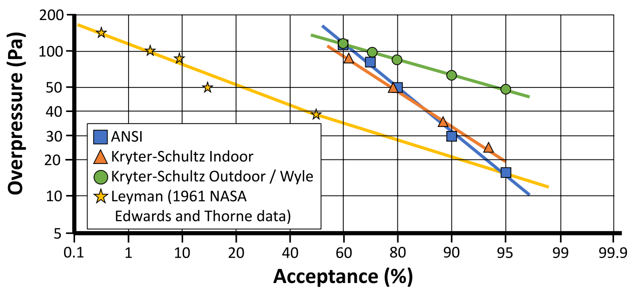

Fig. 7 Sonic boom acceptance according to studies, adapted from [1]

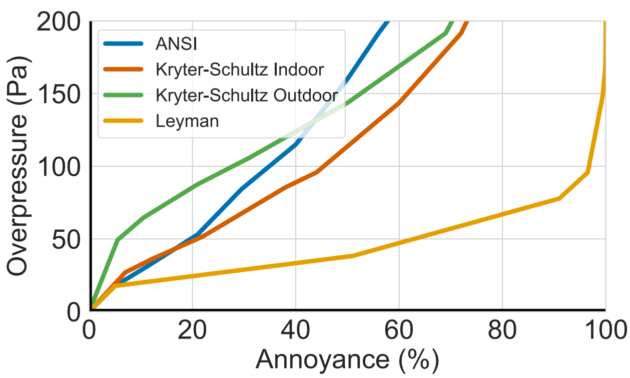

Fig. 8 Sonic boom annoyance, adapted from [1]

be given and a methodology for determining the population disturbance is described.

The three sonic boom parameters have a varying degree of impact on the human response. The overpressure level is the most important, as it correlates with volume, the rise time is mainly responsible for the startling effect and the duration has little effect. Because the rise time is characteristic for each vehicle, it cannot be analysed in this simplified analysis. Thus, the human response will solely be judged on the peak overpressure experienced in a certain geographical area.

The results of previous studies for sonic boom population acceptance in the 1960s and 1980s are displayed in Fig. 7. Because the scaling of the 'Acceptance' in the horizontal axis is non-intuitive, it is adapted for a new display in Fig. 8. Also, for easier computation of the disturbed people, 'Acceptance' is inverted to 'Annoyance'. This was already done reversely for some of the studies in the previous picture, and thus it should be acceptable to convert it back again. These population disturbance models are based on a continuous exposure of one to eight overpressure events per day. Thus, this data should be regarded as broad estimations and not fixed values. Additionally, the overall amount of available data is low and mostly based on US studies from the 1960s and 1980s.

Within the next few years, NASA is planning to perform test flights with its 'quiet supersonic' demonstrator plane X-59 which shall also gather community response [28]. This could give the research area an updated look into the public reaction to regular supersonic flight today.

At first glance, the four curves differ significantly. Until about 130 Pa, Wyle's interpretation of the Kryter–Schultz data is the most benign. While only about 5% are annoyed at 50 Pa, the curve then slopes down and annoyance per Pa increases. The other three curves are assumed almost identical below 20 Pa, although only Leyman is displayed in the original source. Beyond that, the Kryter–Schultz Indoor and ANSI (American National Standards Institute) data points first follow similar patterns until they diverge above 50 Pa. ANSI crosses the Kryter–Schultz Outdoor/Wyle curve at 130 Pa and is beyond that point of the curve with the lowest annoyance values. Finally, Leyman's interpretation of the available data significantly differs from the other three beyond 20 Pa. Already at about 35 Pa, an annoyance ratio of 50% is reached. At 100 Pa, the annoyance ratio is over 95%. While the original source diagram is not very clear at the diagram's edge, an annoyance ratio of almost 100% can be assumed for 200 Pa.

Meta-analyses of this data [29, 30] indicate that the Leyman curve substantially overestimates the number of annoyed people as it diverges profoundly from the other curves. While population annoyance of three curves will be shown (ANSI, Kryter–Schultz Outdoor/Wyle and Leyman), the meta-analyses indicates that ANSI draws the most realistic picture, although slightly conservative in the lower overpressure ranges. Therefore, ANSI will be used as the primary reference in the following analysis.

3.3 Computation of the sonic boom carpet

The previously discussed theory shall be applied to SpaceLiner trajectories and the other comparison vehicles. The computation of the sonic boom for a specific vehicle is based on H.W. Carlson's theory for a simplified sonic boom prediction [31]. It can be found as the reference paper for a number of other sonic boom prediction studies, most notably the FAA (Federal Aviation Administration) environmental review for SpaceX Starship [32]. This theory was implemented into a tool called SALES which was validated based on actual recorded Space Shuttle sonic boom overpressure data [8].

The procedure computes three main values for an N-shaped sonic boom: bow-shock overpressure Δp_{max}, boom duration Δt and lateral extent $d_{y,c}$. The applicable high-level Eqs. (1) to (3) are shown below:

$$\Delta p_{max} = K_{pKR}\sqrt{p_{vpg}}\left(M^2 - 1\right)^{1/8} h_e^{-3/4} l^{3/4} K_S \tag{1}$$

$$\Delta t = K_t \frac{3.42}{a_v} \frac{M}{\left(M^2 - 1\right)^{3/8}} h_e^{1/4} l^{3/4} K_S, \tag{2}$$

$$\mathrm{d_{y,c}} = \mathrm{K_{d,c}} \frac{\mathrm{h}}{\mathrm{M}} \sqrt{\frac{\mathrm{M}^2 - \mathrm{M}_c^2}{\mathrm{M}_c^2 - 1}} \tag{3}$$

with the following parameters: K_p: pressure amplification factor, K_R: reflection factor, p_v: atmospheric pressure, p_g: atmospheric pressure at ground level, M: vehicle Mach number, h_e: effective altitude, l: vehicle characteristic length, K_S: vehicle shape factor, K_t: signature duration factor, a_v: speed of sound at vehicle altitude, $K_{d,c}$: Ray-path distance factor for cutoff conditions, h: vehicle altitude above ground, M_c: vehicle cutoff Mach number below which sonic boom will not reach ground.

While a detailed description of all these factors can be found in [31], the vehicle design and trajectory have a tremendous impact on the equations (l, $\mathrm{K_S}$ and M, h, $\mathrm{h_e}$, respectively).

Specifically, the vehicle shape factor $\mathrm{K_S}$ is calculated by using Whitham's function [33] (see Fig. 9) which depends largely on the effective cross section along the Mach plane. To calculate this, the tool performs multiple cuts of the geometry along the Mach plane and evaluates the area as well as the lift.

The vehicle input is based on a 3D grid displaying the geometry and the pressure distribution for the lift calculation. The pressure distribution was calculated with the DLR tool Hotsose using surface inclination methods. For the comparison vehicles, these meshes are created based on publicly available data. The employed method employed to calculate the $\mathrm{K_S}$ coefficient has convergence problems for very large angles of attack. This primarily impacts Starship and Dream Chaser with their high angle of attack during re-entry. For Starship, an alternative calculation can be performed with a constant K_S of 0.2 as indicated in [32] as the estimated value by SpaceX.

Generally, the sonic boom propagation is only computed for the descent part of the flight after all engines have shut down. It is not possible to determine the vehicle shape factor for the ascent easily with the available methods, as not only the vehicle geometry must be considered but also the shape of the engine exhaust which is ever changing due to the decline in atmospheric pressure during ascent.

For more detailed information on the computation formulas, refer to [31].

While the baseline equations compute the maximum overpressure and the carpet's lateral extension, the actual overpressure decreases towards the edge of the carpet (see Fig. 5). Consequently, the reduction in overpressure at off-track locations is calculated based on a ray-inclination approach suggested by the literature. To limit the computation time and allow a conservative approach, the lateral extension is discretized to five steps each (see Fig. 10). Thus, each rectangle represents the expected sonic boom overpressure between two flight points. Finally, a carpet is spanned along the flight trajectory with a detailed characterization of the local sonic boom overpressure (see Fig. 11).

3.4 Computation of population disturbance

Having estimated the overpressure distribution along the trajectory sonic boom carpet, the population disturbance studies can be applied to all locations.

First, to know the local population count around the whole world, a population database called GPWv4 (Gridded Population of the World, Version 4) is used. It is managed and maintained by NASA's Socioeconomic Data and Applications Center and the Center for International Earth Science Information Network at Columbia University [34]. The data

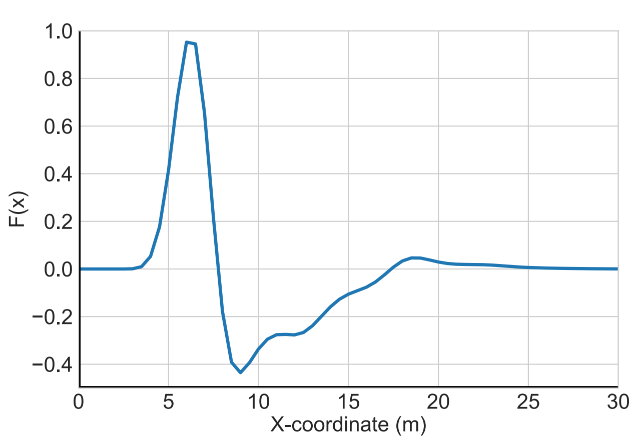

Fig. 9 Whitham's function example result

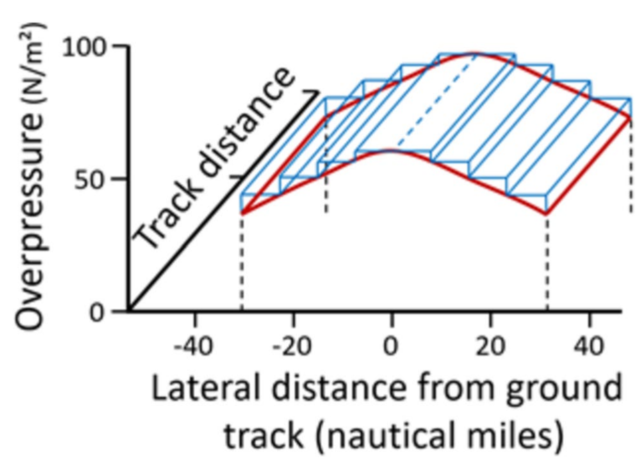

Fig. 10 Schematic drawing showing the discretization of the sonic boom carpet

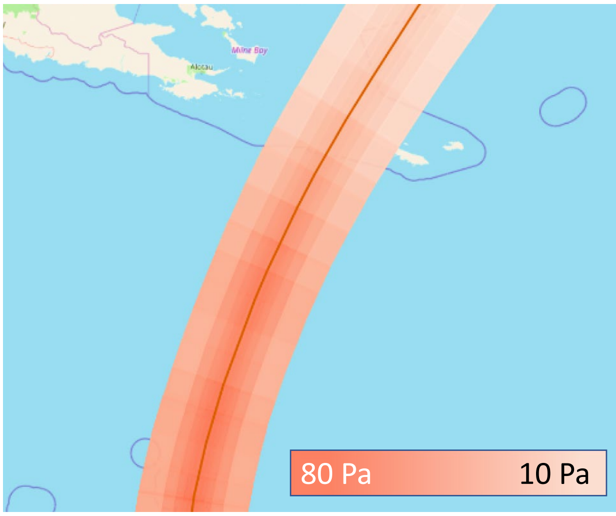

Fig. 11 Discretization of an exemplary sonic boom carpet overlaid on map. Higher colour intensity showing higher sonic boom overpressure

is organized in a gridded form along longitudes and latitudes in a maximum resolution of 30 arc-seconds (approximately 1 km at the equator). As this application does not require such a high precision, a lower resolution of 2.5 arc-minutes is chosen (about 5 km at the equator). An exemplary view of the population density map in this resolution can be seen in Fig. 12.

The overall quality of this data is considered to be good, as it provides values for the whole Earth and can be easily used and implemented. However, it shall be mentioned that in some countries — especially ones with large land area — the data is not as detailed. In these cases, large areas have the same population density data value in the database. Thus, it can be assumed that the number of people living there is averaged for a whole region. As this is primarily done in areas with few people, it is not considered to be problematic for this study.

Along the whole flight trajectory, the population density within the sonic boom area is computed in steps of at maximum 5 km (along and lateral to the flight track) to gain sufficient accuracy in the grid. For each 5 km grid rectangle, the actual local population that is hit by a sonic boom is calculated by multiplying the area with the population density.

Finally, knowing the amount of people living in a place and the local expected overpressure, the disturbance studies are applied to estimate the share of people who will be disturbed by routine sonic booms.

To investigate the overall impact on the world population of one flight, the integral of the population along the flight track and to the side is calculated. The same is done with the share of disturbed people. As a result, both the overall number of people and the estimated number of disturbed people can be calculated for each flight. Given its generally negative impact on the population, these values shall be as low as possible.

4 Results

In this section, the results of the study are presented. At first, the results of the DLR SpaceLiner concept are shown, which include the sonic boom propagation and expected population disturbance. Based on the trajectory analysis performed in [27], a large number of potentially feasible SpaceLiner routes around the world were identified.

Second, the SpaceLiner sonic boom characteristics of a few selected flight routes are compared to the other hypersonic vehicles described previously.

Fig. 12 GPWv4 Population density map of Europe, normalized between 1 and 10 000 people/km^2

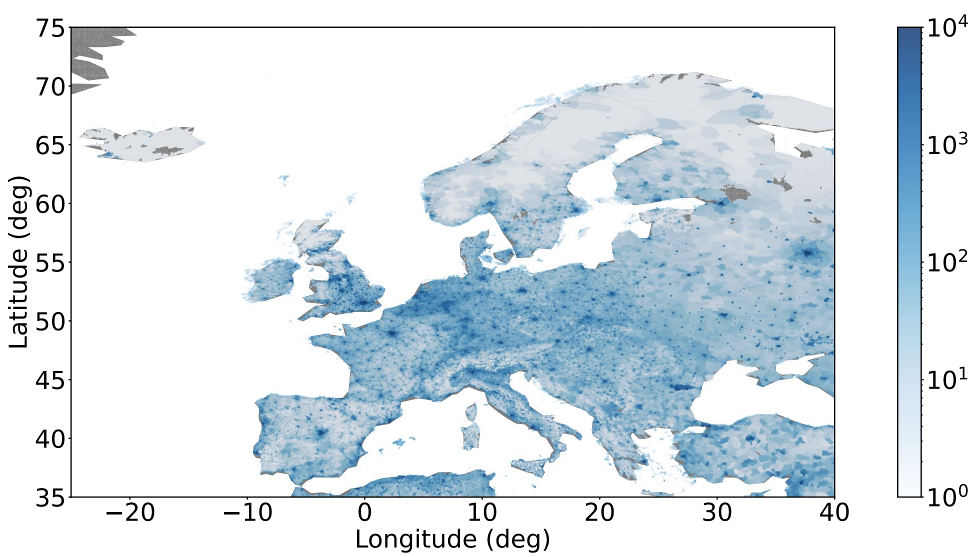

4.1 SpaceLiner

Due to its characteristic flight path with a long gliding flight through the atmosphere, the SpaceLiner is generally prone to a large sonic boom impact area. In Fig. 13, the exemplary route Australia to Virginia, US, is shown with the sonic boom nominalized between 0 and 100 Pa for better visualization. The shown sonic boom carpet is displayed in its actual size on the projected map. Additionally, Fig. 14 shows the expected impact on the population along this route. In total, about 2 million people are overflown on this route, of which 194 000 are expected to be annoyed according to ANSI (ranging from 65 000 for Kryter–Schultz Outdoor/Wyle to 620 000 for Leyman). With these numbers, the Australia–Virginia, US trajectory is positioned at the higher end of the disturbance spectrum.

The flight leaves Australia on a north–north-eastern trajectory over the mostly empty Pacific Ocean. During this part of the flight, the sonic boom overpressure is almost zero and only a small fraction of people are impacted, primarily in the Solomon Islands. Afterwards, it traverses Alaska, northern Canada and the Hudson Bay before turning south again and flying along the Canadian–US border at its most easterly point between Maine (US) and New Brunswick (Canada). In Alaska and northern Canada, the overpressure is still quite low, which is why only a few hundred to thousand people are expected to be negatively affected, mainly in the small city of Fairbanks. Around Hudson Bay, the critical overpressure value of about 20 Pa is exceeded, after which significant disturbance of the population can be expected. This is primarily the case along the border with a high population density and overpressures around 50–60 Pa. As a consequence, the area is shaded dark red in Fig. 14. The final

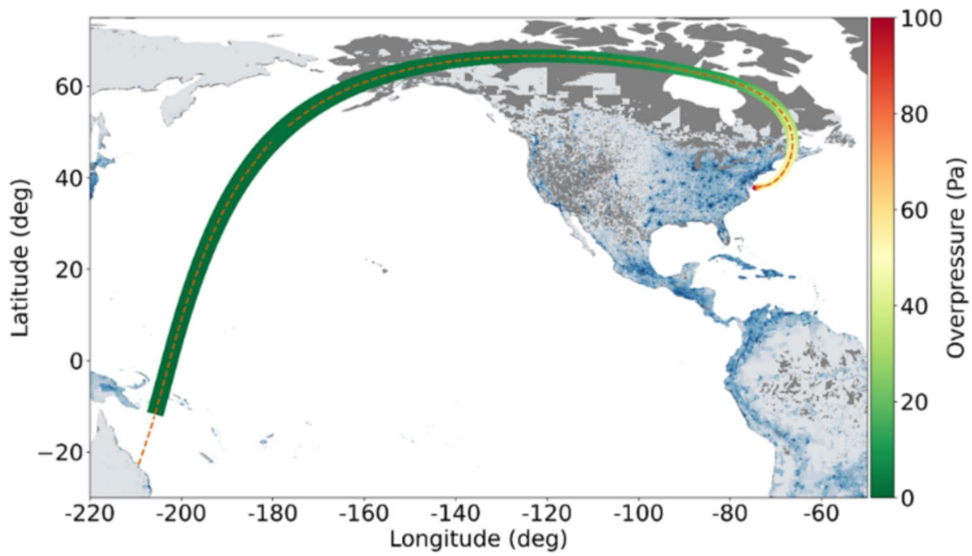

Fig. 13 SpaceLiner sonic boom overpressure on route Australia – Virginia, US (normalized between 0 and 100 Pa)

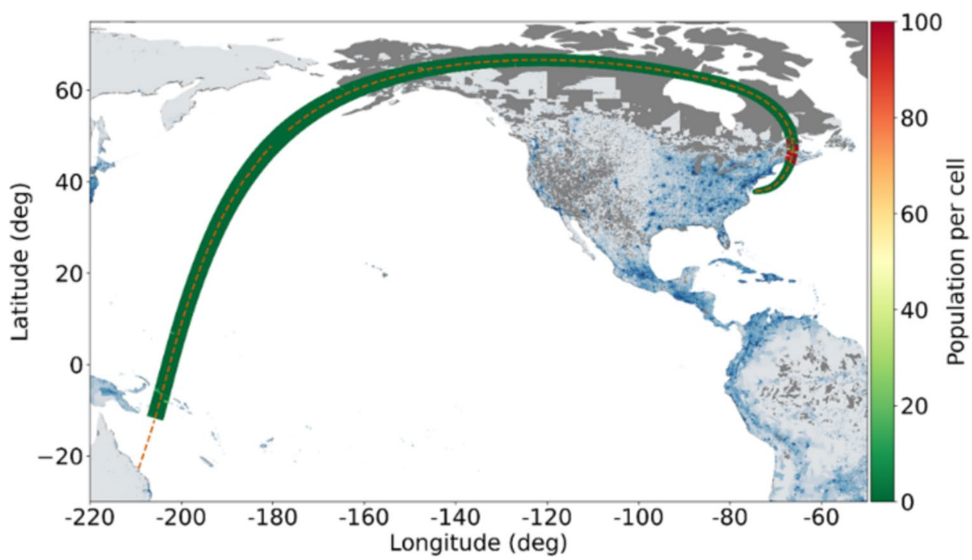

Fig. 14 SpaceLiner sonic boom population disturbance on route Australia - Virginia, US (normalized between 0 and 100 people per cell)

flight phase goes sufficiently far east of the Atlantic coast to avoid overflying any people until it reaches its destination Wallops flight facility in Virginia, US. At the destination, the vehicle transitions to speeds below the speed of sound over the ocean before arriving on land.

A total of 23 envisioned trajectories are shown in Fig. 15, all of which shall connect major economic centres around the world. Generally, most of the trajectories are able to mostly avoid continental landmasses. Only the landmasses near the polar regions are regularly overflown, but this is not considered to be problematic due to the low population density in these areas. Around the equator, two flights go relatively direct from west to east: Florida, US – India and South Africa – California, US. These flights are not able to avoid the population by using the oceans or polar regions. Instead, they cross Africa and the islands of Indonesia, however always at high altitudes and consequently low sonic boom overpressures.

Comparing the worst-case population disturbance values for all routes, there are stark differences of multiple magnitudes immediately identifiable (see Fig. 16). 18 out of 23 routes have a worst-case value below 100 000 people, with 10 of those being below 10 000 people. All of these routes are considered uncritical at this point.

There are two routes with a worst-case value of approximately 200 000 people. Finally, there are three flight routes with disturbed people above 500 000 when using the Leyman study as reference, which heavily penalizes values above 20 Pa.

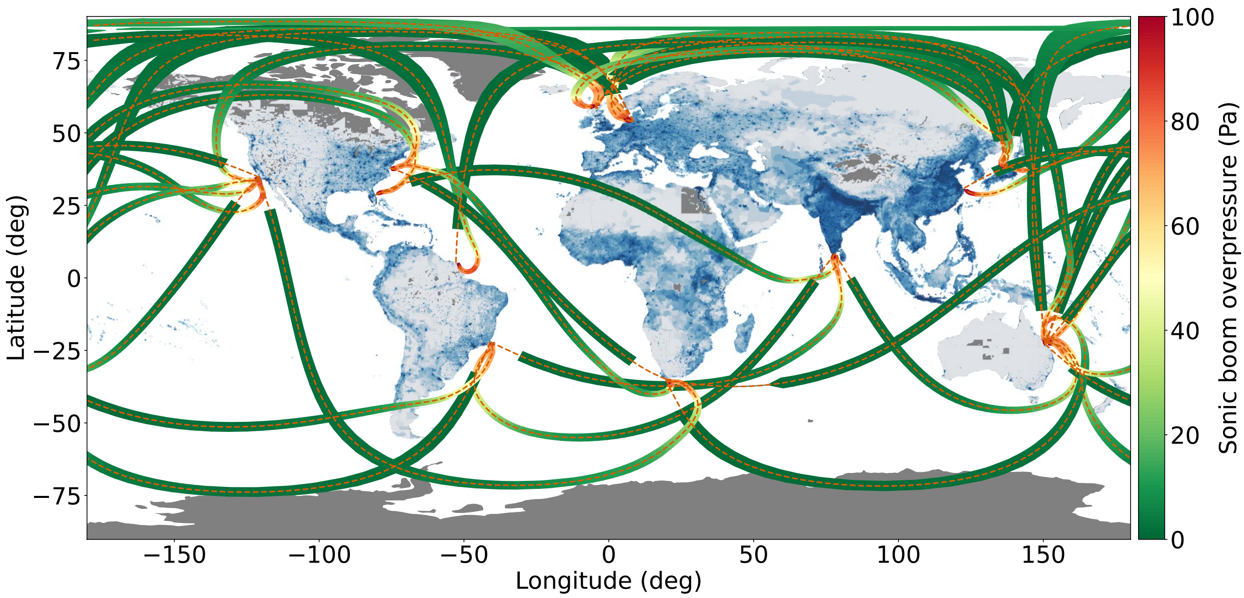

Fig. 15 World map with a selection of envisioned SpaceLiner routes and their sonic boom overpressure (normalized between 0 and 100 Pa)

Fig. 16 Estimated population disturbance by different studies of all envisioned SpaceLiner routes

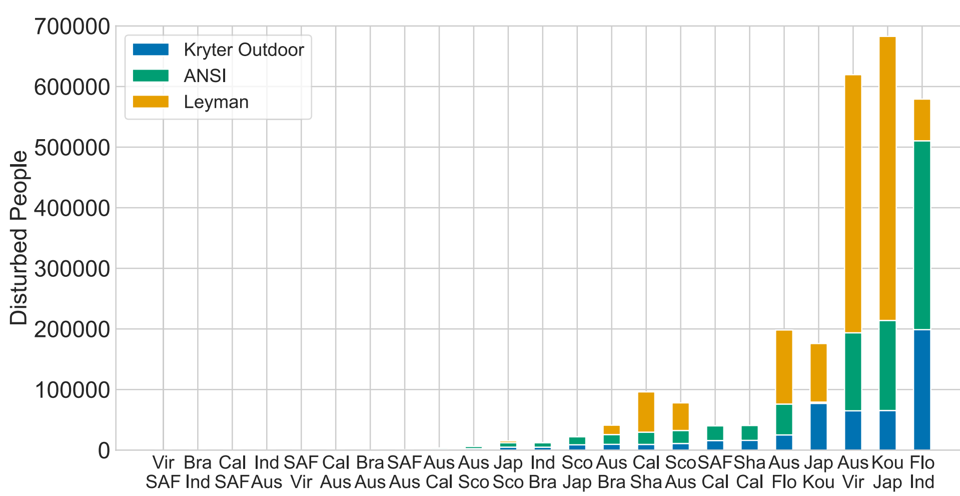

To put these numbers into perspective, an investigation by the British Civil Aviation Authority showed that for the year 2013, around 264 000 people lived within an area surrounding the airport London Heathrow that experienced noise levels responsible for 'significant community annoyance'. [35]

In Fig. 17, the same data for the ANSI columns is shown categorized by the sonic boom overpressure. It can be seen that for most flight routes with high annoyance, the majority of the sonic booms is experienced above 20 Pa. Only for Florida – India, the high-altitude flight over Africa leads to a significant disturbance estimation below overpressures of 20 Pa. In turn, the total overflown population must be very high, because below that threshold only a maximum of 5% of the population is estimated to be annoyed.

This can be seen in Fig. 18 with a logarithmic vertical axis. It shows the overall people experiencing the sonic boom. However, only a part of these people will experience the sonic boom as a disturbance. Because of the logarithmic axis, the bars must be closely analyzed, as the values for the not-disturbed people are usually 1–2 magnitudes higher than for the disturbed. Close to 80 million people are overflown on the flight from Florida to India representing about 1% of the Earth's population. With a peak population disturbance of about 600 000 people, this represents less than 1% of the population flown over on that flight. In contrast, most flight routes overfly between one and ten million people. Additionally, a few trajectories are able to use the oceans and polar regions very efficiently and avoid almost any population and stay below 10 000 or even 1000 people for the descent.

In Fig. 19, the overall impacted area of the primary sonic boom is shown. For SpaceLiner, this area is between 2 and 6.5 million km^2. With a total surface area of Earth of about 510 million km^2, the SpaceLiner impacts about 1.3% of the Earth in the worst case. For all trajectories, the large majority of the impacted area experiences a sonic boom below 20 Pa. Only in the final part of the flight, when the vehicle is at lower altitudes and speeds, higher overpressures reach the ground.

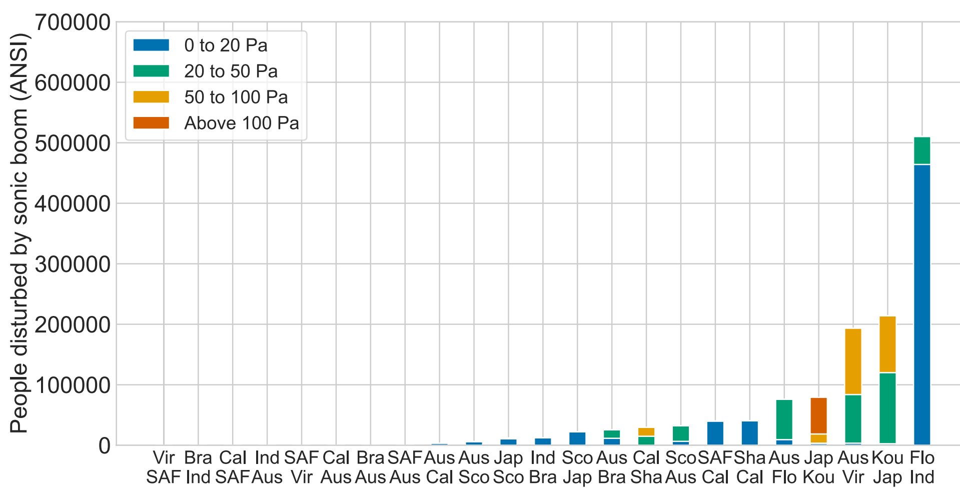

Fig. 17 Estimated population disturbance (ANSI) by sonic boom overpressure range of all envisioned SpaceLiner routes

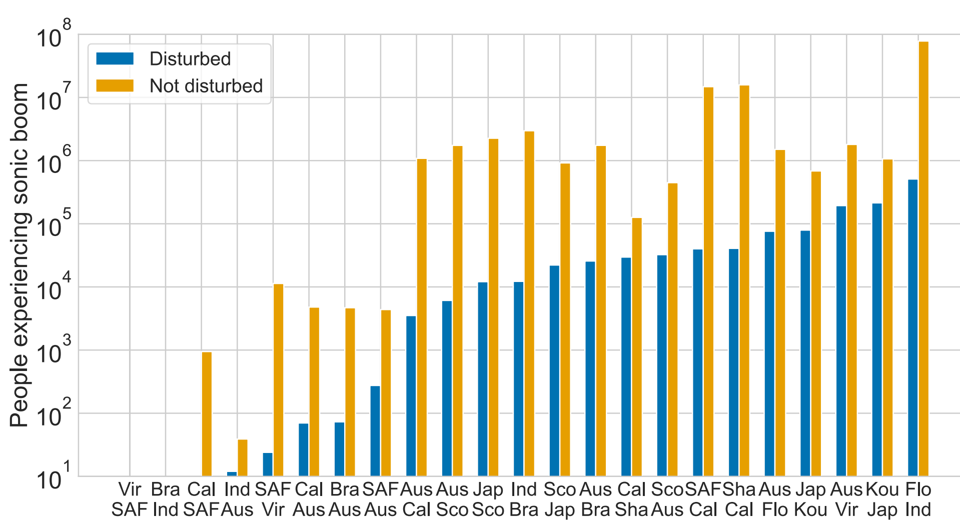

Fig. 18 Estimated population experiencing sonic boom by disturbance of all envisioned SpaceLiner routes on a logarithmic scale

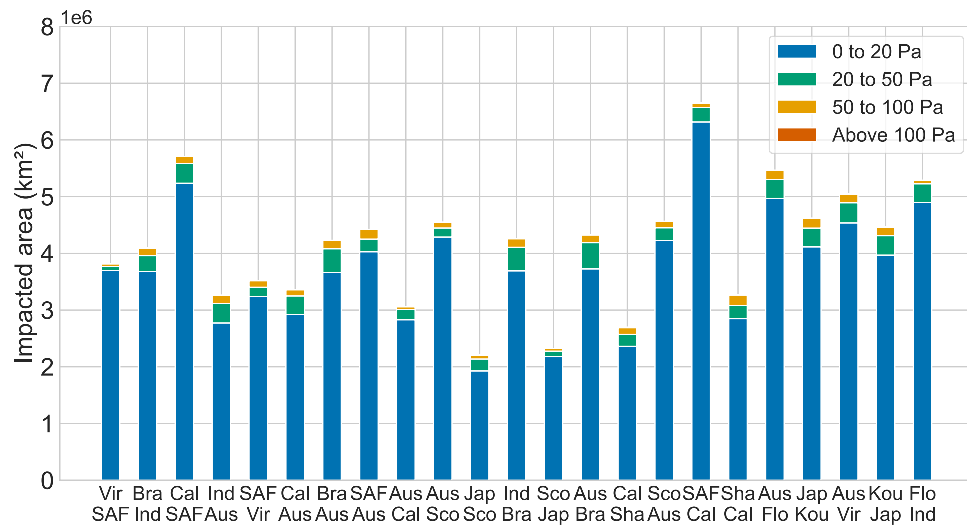

Fig. 19 Impacted area by sonic boom overpressure of all envisioned SpaceLiner routes

4.2 Comparison to other vehicles

For each vehicle, a reference trajectory is used which represents the general characteristics of the mission. These are as follows and are displayed in Fig. 20:

- SpaceLiner routes: Australia – Virginia, US (reference); South Africa – California, US (longest route); Scotland – Japan (shortest route).
- Starship: re-entry to Boca Chica, US.
- Dream Chaser: re-entry to Rostock, Germany.
- Space Rider: re-entry over the Pacific comparable to the IXV test flight.
- Aurora: re-entry after launch from Kourou to polar orbit.

The SpaceLiner flight routes are quite unique due to its high hypersonic lift-to-drag ratio, which lets it fly long distances at high altitudes. These characteristics lead to the results discussed in the previous section. Because most other hypersonic vehicles do not have such a long gliding phase, the sonic boom characteristic are expected to be different, too. Thus, the previously discussed vehicles Starship, Dream Chaser, Space Rider and Aurora are herein compared to a selection of the SpaceLiner trajectories, which showcase a broad range of trajectories from short to long range.

For Starship, Dream Chaser and Space Rider, the reference trajectory is an orbital re-entry. Thus, these will enter the atmosphere with high speeds of about Mach 25 and a shallow flight-path angle of about -1 degree at the

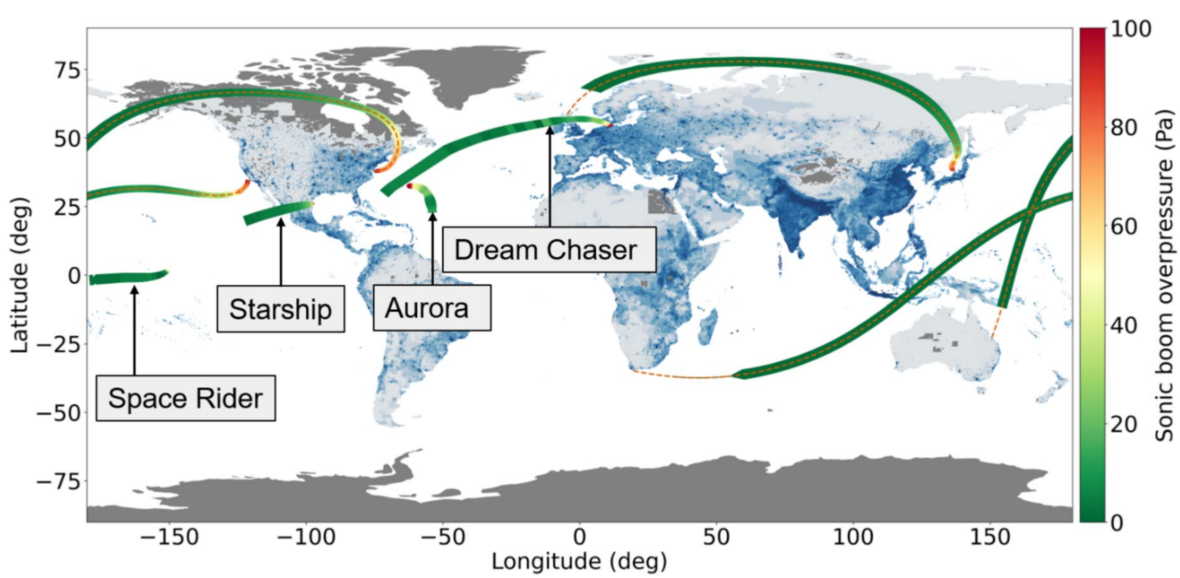

Fig. 20 World map with the routes selected for comparison and their sonic boom overpressure (normalized between 0 and 100 Pa)

beginning of the sonic boom flight interface at an altitude of 80 km. For Aurora, the first stage descent after a launch is investigated. Initially, the vehicle flies with a speed of Mach 15. Due to the lower speed, it re-enters the atmosphere with a higher flight-path angle of about – 5 degrees.

Figure 21 shows an assessment of the impacted sonic boom area depending on the overpressure magnitude. While it was established that the SpaceLiner impacts an area between 2 and 6.5 million km^2, the other vehicles all affect a smaller area. Only the Dream Chaser re-entry impacts an overall area of 2.3 million km^2, which is equal to a SpaceLiner mission from Scotland to Japan. Due to Starship's and Space Rider's quick deceleration in the atmosphere, they merely impact 0.9 million km^2 and 1.1 million km^2. Aurora, which flies significantly slower, affects about 450 000 km^2.

Analysing the magnitude of the overpressure on the impacted area, it can be seen that the long-range SpaceLiner missions vary between 150 000 km^2 and 400 000 km^2 for overpressures above 20 Pa, which are most critical for population disturbance. The other vehicles impact less area at these overpressure levels: 23 000 km^2 for Starship, 58 000 km^2 for Dream Chaser, 5 000 km^2 for Space Rider and 132 000 km^2 for Aurora.

Generally, this indicates that less population would be annoyed by the other vehicles. However, the vehicles' flight characteristics are very different. While for example Starship impacts less area per re-entry overall and also in the high overpressures, it is limited in its route choice with almost no cross-range capability. Winged vehicles like the SpaceLiner or Dream Chaser impact more area, but can use their wings to divert around populated landmasses if performance permits.

In Fig. 22, the sonic boom overpressure is shown over the downrange distance. At high altitudes in the beginning of the flight, all vehicles have low overpressures. Depending on the re-entry profile, the increase is either shallow or steep.

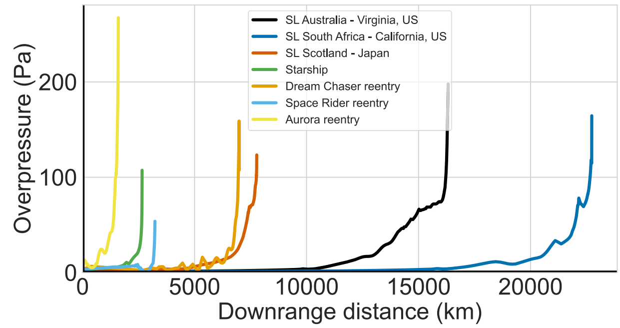

Fig. 22 Overpressure to downrange distance for a selection of the envisioned SpaceLiner trajectories in comparison to the other vehicles

The SpaceLiner trajectories stay at very low overpressures for a long time. In the case of the route South Africa – California, US, the overpressure is insignificant for the first 15 000 km of travelled distance. Later, the overpressure gradually increases to a level of about 75 Pa, where it stabilizes shortly. In the final phase of the flight, the overpressure increases to its peak value between 125 and 200 Pa.

The Dream Chaser data follows a similar pattern to the SpaceLiner route Scotland – Japan in the beginning. Because the available trajectory is skipping and the vehicle's high angle of attack during re-entry causes numerical problems as discussed in Sect. 3.2, there is some variance in the overpressure in the first part of the flight. It diverts at the end with a very steep increase to maximum overpressure. Starship and Aurora have similarly steep increases at the end of the flight with an almost vertical line. This shows why the impact area with high overpressures is lower for these

Fig. 21 Impacted area by sonic boom overpressure for a selection of the envisioned SpaceLiner routes in comparison to the other vehicles

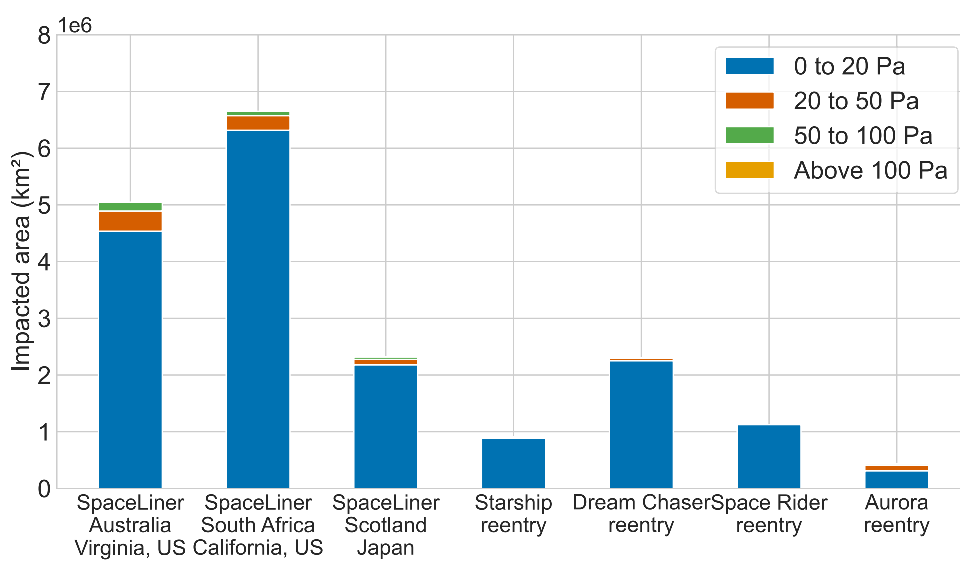

cases. While Space Rider also experiences a steep increase at the end, the peak overpressure only slightly exceeds 50 Pa. This can mainly be traced back to the vehicle size and shape which creates less lift than the other vehicles.

These considerations are supported by the diagram in Fig. 23, which shows the overpressure over altitude. Initially, it can be easily seen that the Aurora re-entry profile differs noticeably. It has substantially higher overpressures at altitudes below 50 km, which can be most likely traced back to its size and the steep re-entry.

Above 30 km and below 55 km, the Space Rider generally has the lowest overpressure of all vehicles. Second in line is Dream Chaser, which, apart from Space Rider, is notably smaller than the other vehicles and at 55 km altitude switches from an angle of attack of 45 degrees to 20 degrees. The SpaceLiner is in the middle of the fleet with a moderate increase to about 75 Pa until 30 km altitude. While Starship's overpressure is slightly higher than SpaceLiner at 50 km, it is only about 60 Pa at 30 km.

Dream Chaser and Starship follow a similar pattern below 30 km. Only the peak overpressure is approximately 50% higher for Dream Chaser although it is significantly smaller. Because it flies supersonic at lower altitudes, the peak overpressure is higher. It seems to be advantageous to transfer from super- to subsonic at the highest altitude possible.

With a peak overpressure of about 107 Pa for Starship, the values are in line with the FAA Environmental Assessment data provided by SpaceX [32] for a landing in Boca Chica, US (peak overpressure of 2.2 lbf/ft^2 or 105.3 Pa).

A more detailed comparison of six flight conditions is shown in Fig. 24. Each diagram shows the lateral overpressure distribution at specific altitudes from 70 to 20 km (or the point of maximum overpressure when the transition to subsonic is above 20 km).

Generally, the SpaceLiner curves stay relatively constant over all diagrams even though they achieve widely different downrange distances. This showcases that the main flight difference for these missions occurs above 60 km,

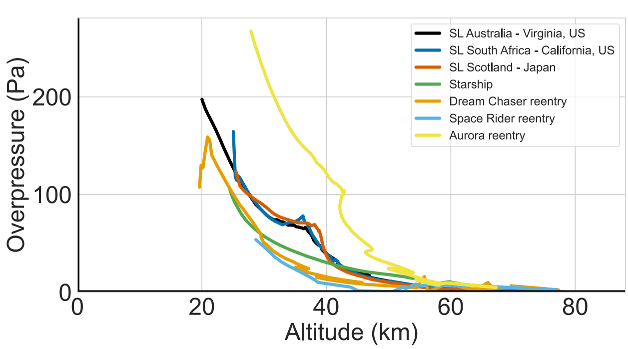

Fig. 23 Overpressure to altitude for a selection of the envisioned SpaceLiner trajectories in comparison to the other vehicles

where higher initial speeds lead to long glides with low overpressures. The arrival at the destination and the associated increase in overpressure while decreasing the altitude is relatively similar for all SpaceLiner missions. In the 60 and 70 km altitude range, the other vehicles have two to three times higher overpressures than SpaceLiner. However, because the overall magnitude of the sonic boom is below 10 Pa, this does not make a large difference on the population disturbance. The primary reason for this discrepancy is presumably the lower flight-path angle for the re-entry missions (larger than −1 degree vs. smaller than −0.2 degrees). In this phase, the lateral extents of the sonic booms are the largest between 150 and 190 km in either direction.

At 50 km, the overpressures of the Dream Chaser and Space Rider are a few Pa lower than at 60 km. For Dream Chaser, the previously mentioned skipping trajectory creates a certain amount of variation that should be considered. Additionally, at 55 km altitude, the Dream Chaser changes angle of attack from 45 to 20 degrees. At 45 degrees, the tool runs into some numeric problems when calculating the vehicle shape factor K_S which is applicable for both vehicles. Thus, the Dream Chaser values above 55 km should be considered with higher uncertainties.

While the SpaceLiner trajectories only experience peak overpressure values of about 10 Pa at 50 km, Starship is at about 19 Pa peak overpressure, whereas Aurora is already at about 24 Pa. The lateral extent of all vehicles is reduced to about 90 km in either direction.

At 40 km, Aurora is already in the steep re-entry phase described before with a peak overpressure of 120 Pa. Starship and SpaceLiner are close together between 35 and 40 Pa, while Dream Chaser and Space Rider are still below 20 Pa.

At 30 km, Aurora is already close to the subsonic transition with a small lateral sonic boom width of 40 km total and overpressures well beyond 200 Pa. At this point, the other vehicles are still below 100 Pa and a total lateral extent of about 120 km.

The last image shows the overpressure distribution either at 20 km altitude or at the peak overpressure shortly before transitioning to subsonic speeds. For Aurora, the peak overpressure of over 250 Pa is reached at about 27 km. The chosen SpaceLiner routes have a maximum overpressure of 200 Pa. Starship peaks at approximately 107 Pa at 24 km altitude. The lateral expansions are generally below 100 km in total and decrease rapidly in this flight phase.

Finally, Fig. 25 displays the estimated population disturbances of the compared vehicles and routes. Although their status is referred to as reference trajectory, this might not reflect an operational trajectory. This is especially the case for the Space Rider re-entry which was based on the IXV test article and landed in the Pacific Ocean. In real operations, it would land in Kourou, the Azores Islands or Italy.

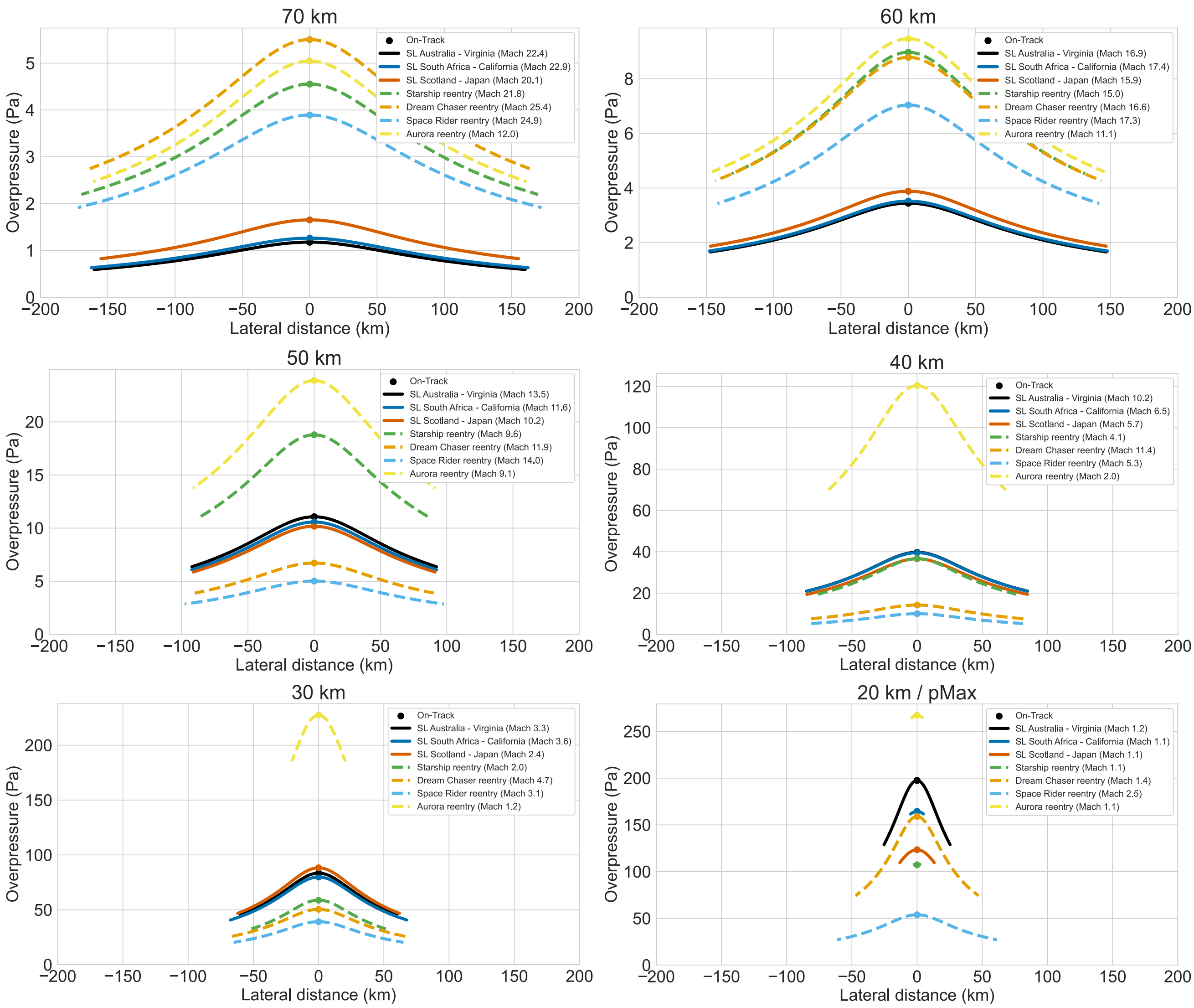

Fig. 24 Lateral overpressure distribution at altitudes between 20 and 70 km for a selection of the envisioned SpaceLiner trajectories in comparison to the other vehicles

The Starship re-entry is considered the most realistic as it assumes landing at the SpaceX Starship facility in Boca Chica, US, as is planned by SpaceX. It arrives from the west with an initial inclination of 27.5° (see Fig. 20). Therefore, it could resemble a vehicle that has been launched from Boca Chica and arrives there as well. Because it flies over Mexico, almost 1 million people are expected to be disturbed which is the highest out of all trajectories.

Dream Chaser re-enters over Scotland as well as Denmark plus northern Germany. That is why it also has such a high annoyance value of about 550 000 people.

5 Discussion

The results show that the SpaceLiner and also the other vehicles create a substantial sonic boom carpet along their flight track. For regular operations, the negative impact on the population must be minimized as much as possible.

First, this includes the trajectory design, which should avoid populated areas as much as possible and ideally utilize the vast open water areas of the Oceans during the majority of the flight. It is shown that when the optimizing process considers the population data, a large number

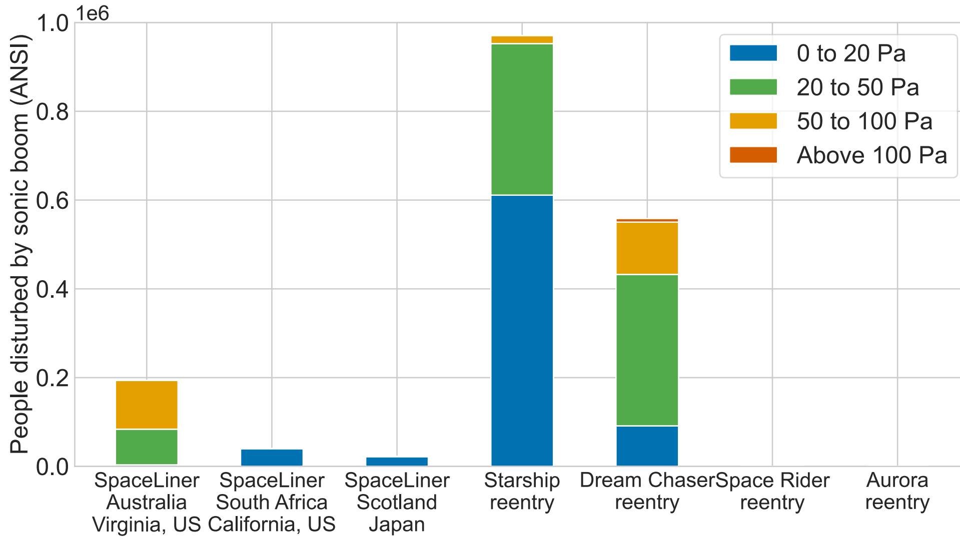

Fig. 25 Estimated population disturbance by sonic boom overpressure range for a selection of the envisioned SpaceLiner trajectories in comparison to the other vehicles

of SpaceLiner routes are found which are expected to disturb a very small number of people, especially when compared to the overall area that is flown over. Additionally, the flexibility of the methodology is shown by application to four different hypersonic vehicles.

Second, the results of this work shall flow into the early design process. Beyond the scope of this paper, there has been work on the next generation of the SpaceLiner passenger stage, version 8. One of the main high-level requirements was that the vehicle shall additionally be able to perform missions ‘skipping’ over territories after the ascent phase. This is intended for large conglomerations of people living within the extended launch ascent path. This requirement was a direct outcome of the results from this study.

Initial results show that for the reference trajectory Australia – Europe, the impacted population can be reduced by 98% [36]. In contrast to the SpaceLiner 7 trajectory, the people living in Oceania (e.g. the Solomon’s) do not experience a sonic boom as the vehicle travels outside of the atmosphere in this flight phase.

This example shows how this work has already fed back into the high-level requirements and therefore design of the next generation vehicle studies. It shall be underlined that such a big change is only possible in the early concept design phases. Consequently, such a study can deliver important decision points within the design phase. However, it shall also be mentioned that this methodology is limited to the trajectory design of the sonic boom. Another important factor for the sonic boom is the shape optimization which is not done within the scope of this study and is generally limited for hypersonic vehicles due to other factors like aerothermodynamics.

6 Conclusion

The creation of sonic booms is a central part of super- and hypersonic travel. The analysis of the sonic boom propagation of hypersonic vehicles shows a significant impact on the ground area along their flight tracks.

The detailed analysis of the SpaceLiner flight routes shows that over 1% of the Earth’s surface can be impacted. However, most of this area is affected only with a small overpressure event. Due to its wings, it is able to fly around populated landmasses and avoid high disturbance of the population living below. Up to 600 000 people are expected to be disturbed in the worst-case SpaceLiner route, while almost all envisioned routes stay below 100 000 people and almost half even below 10 000.

Comparing the SpaceLiner to other vehicles, the impacted area is lower for the other vehicles, most of which do not utilize a high lift-to-drag ratio for a prolonged glide in the upper atmosphere. The peak sonic boom overpressure varies depending on vehicle size and trajectory between 50 and 250 Pa. The sonic boom impact is important for population acceptance, especially when flying regularly. This is especially the case for vehicles which are limited in using their lifting capabilities to diverge around populated landmasses (e.g. Starship, Space Rider). The availability of re-entry or point-to-point routes might be severely limited depending on the regulatory framework.

Because the methodology used in this study to compute the overpressure is based on simplified assumptions, the results should be viewed as such. It is intended as a tool for early design phases and not to accurately determine the overpressure for e.g. regulatory approval. Furthermore, the population surveys used in the acceptance studies are quite old and might lead to different results if repeated today.

For future research, it would be beneficial if the sonic boom propagation were to be implemented directly within the trajectory optimization, as the population avoidance manoeuvres are currently performed based on an estimated lateral extension of the sonic boom. However, at this point in time it requires too much computational resources to be feasible. Furthermore, there should be more effort concerning the identification of suitable spaceports such that the population disturbance can be reduced to a minimum.

The work of this study has already fed back into the requirements of the next generation SpaceLiner vehicle and initial results already show promising results where the amount of people being negatively affected by a sonic boom could be reduced substantially.

Summarizing, this study showcased the importance of considering the sonic boom impact on the trajectory design of hypersonic vehicles in the initial design phase.

Author contribution S.C. performed the majority of the work and writing of the original draft. J.W. contributed to the conceptualization and methodology of the study and performed review and editing of the paper. Additionally, J.W. created the software to perform the sonic boom estimation. M.S. supervised the project and contributed to the conceptualization of the study.

Funding Open Access funding enabled and organized by Projekt DEAL. Part of this work was performed within the project 'European Concept of Higher Airspace Operations' (ECHO). This project has received funding from the SESAR Joint Undertaking (JU) under grant agreement No 890417. The JU receives support from the European Union's Horizon 2020 research and innovation programme and the SESAR JU members other than the Union. Further information on ECHO can be found athttps://higherairspace.eu/

Data availability No datasets were generated or analysed during the current study.

Declarations

Conflict of interest The authors have no relevant financial or non-financial interests to disclose.

References

1. Maglieri, D. J., Bobbitt, P. J., Plotkin, K. J. et al.: Sonic Boom – Six Decades of Research. NASA/SP-2014–622, Hampton, Virginia, USA (2014)
2. King, C. B., Skowron, S., Miller, S. A.: Fully-parabolized prediction of hypersonic sonic boom. AIAA Aviation 2023 Forum, San Diego, USA (2023). https://doi.org/10.2514/6.2023-4167
3. Zou, S., Johnston, Z. M., Candler, G. V., Yang, S.: Rapid hypersonic sonic boom prediction using line-distributed energy impulse formulations with and without lift effect. AIAA SCITECH Forum, National Harbour, USA (2023). https://doi.org/10.2514/6.2023-0816
4. Luquet, D., Marchiano, R., Coulouvrat, F., Salah El Din, I., Loseille, A.: Sonic boom assessment of a hypersonic transport vehicle with advanced numerical methods. 21st AIAA/CEAS Aeroacoustics Conference, Dallas, USA (2015). https://doi.org/10.2514/6.2015-2685
5. Leng, Y., Qian, Z.: Sonic boom signature analysis for a type of hypersonic long-range civil vehicle. 21st AIAA International Space Planes and Hypersonics Technologies Conference, Xiamen, China (2017). https://doi.org/10.2514/6.2017-2244
6. Chernyshev, S.L., Gorbovskoy, V.S., Kazhan, A.V., Korunov, A.O.: Re-entry vehicle sonic boom issue: modelling and calculation results in windy atmosphere based on the augmented Burgers equation. Acta Astronautica **194**, 450–460 (2022). https://doi.org/10.1016/j.actaastro.2021.12.038
7. Loubeau, A., Coulouvrat, F.: Effects of meteorological variability on sonic boom propagation from hypersonic aircraft. AIAA J. **47**, 11 (2009). https://doi.org/10.2514/1.41337
8. Maglieri, D. J., Henderson, H. R., Massey, S. J., Stansbery, E. G.: A Compilation of Space Shuttle Sonic Boom Measurements. NASA/CR-2011–217080 (2011).
9. Sippel, M., Stappert, S., Bayrak, Y. M., Bussler, L., Callsen, S.: Systematic assessment of spaceliner passenger cabin emergency separation using multi-body simulations. 2nd International Conference on High-Speed Vehicle Science Technology (HiSST), Bruges, Belgium (2022)
10. Sippel, M.: Promising roadmap alternatives for the SpaceLiner. Acta Astronautica **66**(11-12), 1652-1658 (2010). https://doi.org/10.1016/j.actaastro.2010.01.020
11. Sippel, M., Trivailo, O., Bussler, L. Lipp, S., Kaltenhäuser, S., Molina, R.: Evolution of the SpaceLiner towards a Reusable TSTO-Launcher. 67th International Astronautical Congress (IAC), Guadalajara, Mexico (2016)
12. Neeb, D., Schwanekamp, T., Gülhan, A.: Preliminary aerodynamic shape optimization of the spaceliner by means of engineering methods. 17th AIAA International Space Planes and Hypersonic Systems and Technologies Conference, San Francisco, USA (2011)
13. Sippel, M., van Foreest, A., Dietlein, I., Schwanekamp, T., Kopp, A.: Analyses Driving improved aerothermodynamic layout of the spaceliner configuration. ESA-SP692 (2011)
14. Sippel, M., Schwanekamp, T.: The SpaceLiner hypersonic system – aerothermodynamic requirements and design process. 8th european symposium on aerothermodynamics for space vehicles, Lisbon, Portugal (2015)
15. Zuppardi, G., Morsa, L., Savino, R., Sippel, M., Schwanekamp, T.: Rarefied aerodynamic characteristics of aero-space-planes: a comparative study of two gas-surface interaction models. Eur. J. Mech. B/Fluids **53**, 37–47 (2015). https://doi.org/10.1016/j.euromechflu.2015.04.003
16. SpaceX: Starship, https://www.spacex.com/vehicles/starship (accessed June 2024)

17. SpaceX (YouTube): Starship Update, 11th February 2022, https://www.youtube.com/watch?v=3N7L8Xhkzqo (accessed June 2024)
18. SpaceX (YouTube): Starship | Earth to Earth, 29th September 2017, https://www.youtube.com/watch?v=zqE-ultsWt0 (accessed June 2024)
19. Wilken, J., Callsen, S.: Mission design for point-to-point passenger transport with reusable launch vehicles. CEAS Space J. (2023). https://doi.org/10.1007/s12567-023-00498-9
20. Wilken, J., Berger, M., Sippel, M.: Critical analysis of SpaceX's next generation space transportation system: starship and super heavy. 2nd International Conference on High-Speed Vehicle Science Technology (HiSST), Bruges, Belgium (2022)
21. Sierra Space: Dream Chaser, https://www.sierraspace.com/space-transportation/dream-chaser-spaceplane/ (accessed June 2024)
22. Kaltenhäuser, S., Klünker, C., Schmitt, D. R., Sippel, M., Veth, J., Zimmermann, K., Lockheed Jr, A. H., Strom, J. R.: Machbarkeitsstudie spaceport Rostock-Laage – executive summary (2020)
23. ESA: To orbit and back with Space Rider, https://www.esa.int/EnablingSupport/SpaceTransportation/Space_Rider/To_orbit_and_back_with_Space_Rider, 2022 Accessed June 2024.
24. Bonetti, D., De Zaiacomo, G., Blanco Arnao, G. Medici, G., Pontijas Fuentes, I., Parreira, B.: Space Rider Mission Engineering. 8th European Conference for Aeronautics and Space Sciences (EUCASS), Madrid, Spain (2019)
25. Kopp, A., Stappert, S., Mattsson, D., Olofsson, K., Marklund, E., Kurth, G., Mooij, E., Roorda, E.: The Aurora space launcher concept. CEAS Space J. **10**, 167–187 (2018). https://doi.org/10.1007/s12567-017-0184-2
26. Polaris Raumflugzeuge: Light Spaceplane Aurora, https://www.polaris-raumflugzeuge.de/Technology/Light-Spaceplane-AURORA (accessed June 2024)
27. Callsen, S., Wilken, J., Stappert, S., Sippel, M.: Feasible options for point-to-point passenger transport with rocket propelled reusable launch vehicles. Acta Astronautica **212**, 100–110 (2023). https://doi.org/10.1016/j.actaastro.2023.07.016
28. Rathsam, J. Coen, P., Loubeau, A., Ozoroski, L., Shah, G.: Scope and Goals of NASA's Quesst Community Test Campaign with the X-59 aircraft. 14th ICBEN Congress on Noise as a Public Health Problem, Belgrade, Serbia (2023)
29. Brown, D., Sutherland, L. C.: Sonic Boom (Human Response and Atmospheric Effects) Outdoor-to-Indoor Response to Minimized Sonic Booms. N94–33502, High Speed Research Workshop, Williamsburg, Virginia, USA (1991)
30. Hubbard, H. H., Shepherd, K. P.: Comparisons of Methods for Predicting Community Annoyance Due to Sonic Booms. NASA Technical Memorandum 110289, Langley Research Center, Hampton, Virginia, USA (1996)
31. Carlson, H. W.: Simplified Sonic-Boom Prediction. NASA Technical Paper 1122, Langley Research Center, Hampton, Virginia, USA (1978)
32. Federal Aviation Administration: Final Programmatic Environmental Assessment for the SpaceX Starship/Super Heavy Launch Vehicle Program at the SpaceX Boca Chica Launch Site in Cameron County, Texas – Appendix B (Noise Assessment). KBR TN 20–02 (2020)
33. Whitham, G.B.: The flow pattern of a supersonic projectile. Commun. Pure Appl. Math. **5**(3), 301–348 (1952). https://doi.org/10.1002/cpa.3160050305
34. Center for International Earth Science Information Network – CIESIN – Columbia University, 2016, Gridded Population of the World, Version 4 (GPWv4): Population Density. Palisades, NY: NASA Socioeconomic Data and Applications Center (SEDAC). https://doi.org/10.7927/H4NP22DQ (accessed June 2024)
35. Civil Aviation Authority: Information on aviation's environmental impact. CAP 1524, West Sussex, UK (2017)
36. Mauriello, T., Callsen, S., Bussler, L., Wilken, J., Sippel, M.: Multidisciplinary Design Assessment of Promising Aerodynamic Shapes for Hypersonic Passenger Transport. 75th International Astronautical Congress (IAC), Milan, Italy (2024).